Charged-hadron suppression in Pb+Pb and Xe+Xe collisions measured with the ATLAS detector

Petr Balek (for the ATLAS Collaboration)

Dept. of Particle Physics and Astrophysics, Faculty of Physics, Weizmann Institute of Science, 234 Herzl Street, Rehovot 76100, Israel

Abstract

The measurement of charged-hadron production in heavy-ion collisions provides insight into the properties of the quark-gluon plasma by measuring parton energy loss. The ATLAS detector at the LHC recorded 0.49 nb^{-1} of Pb+Pb collisions and 25 pb^{-1} of pp collisions, both at the center-of-mass energy 5.02 TeV per nucleon pair. Recently, ATLAS also recorded 3 μb^{-1} of Xe+Xe collisions at the center-of-mass energy 5.44 TeV, which provides a new opportunity to study the system-size dependence of the parton energy loss. The large acceptance of the ATLAS detector allows to measure the charged-hadron spectra in a wide range of pseudorapidity and transverse momentum. The nuclear modification factors R_{AA} are constructed as a ratio of the spectra measured in Pb+Pb or Xe+Xe collisions to that measured in pp collisions. The R_{AA} obtained in the two systems are presented for different centrality intervals and the results are discussed.

Keywords: xenon–xenon collisions, lead–lead collisions, charged-hadron production, nuclear modification factor

1. Introduction

The Xe+Xe collisions delivered by the LHC in 2017 offer a unique opportunity to study properties of the quark-gluon plasma in system with different geometry [1, 2]. Previous measurements show that the yields of charged hadrons are suppressed in the Pb+Pb collisions relative to the pp collisions [3, 4] in a centrality-dependent way. The new Xe+Xe data allow to study the centrality dependence of this suppression at a whole new angle.

The suppression of charged-hadron production is quantified using the nuclear modification factor R_{AA}:

$$R_{\mathrm{AA}} = \frac{1}{\langle T_{\mathrm{AA}} \rangle} \frac{1/N_{\mathrm{evt}} \, \mathrm{d}^2 N_{\mathrm{ch}}/\mathrm{d}\eta \mathrm{d}p_{\mathrm{T}}}{\mathrm{d}^2 \sigma_{pp}/\mathrm{d}\eta \mathrm{d}p_{\mathrm{T}}}, \tag{1}$$

where $\langle T_{\mathrm{AA}} \rangle$ is the nuclear thickness function which accounts for the fact that in a nucleus–nucleus collision, a nucleon can interact with more than one nucleon from the other nucleus; $1/N_{\mathrm{evt}} \, \mathrm{d}^2 N_{\mathrm{ch}}/\mathrm{d}\eta \mathrm{d}p_{\mathrm{T}}$ is the per-event yield of charged hadrons in Xe+Xe or Pb+Pb collisions measured differentially in pseudorapidity η and transverse momentum p_{T}; and $\mathrm{d}^2 \sigma_{pp}/\mathrm{d}\eta \mathrm{d}p_{\mathrm{T}}$ is the differential pp cross-section.

2. Analysis

The measurement [5] described in this proceeding uses Xe+Xe data recorded by the ATLAS detector [6] at $\sqrt{s_{NN}}$ = 5.44 TeV with the total integrated luminosity of $3\,\mu b^{-1}$. The pp cross-section is obtained by extrapolation of $\sqrt{s}$ = 5.02 TeV data [4] to the same center-of-mass energy.

The measurement is performed using the inner detector, calorimeters, muon spectrometer, trigger system and data acquisition system. The tracking information is provided by the inner detector covering $|\eta| < 2.5$. It is immersed in a 2 T axial magnetic field. The calorimeter system consists of an electromagnetic calorimeter covering $|\eta| < 3.2$, hadronic calorimeters covering also $|\eta| < 3.2$ and forward calorimeters covering $3.1 < |\eta| < 4.9$. The muon spectrometer covers $|\eta| < 2.7$. The Xe+Xe events were recorded with two minimum-bias triggers. They required the total transverse energy deposited in the calorimeters to be more than 4 GeV or to have at least one track reconstructed in the inner detector.

The centrality of the collisions is characterized by the total transverse energy in the forward calorimeters (FCal E_T), whose distribution is divided into percentiles of the inelastic cross-section. If the nuclei overlap significantly, the collision is called "central", while collisions with a small overlap are called "peripheral". A Monte Carlo Glauber model simulation [7, 8] is used to estimate the mean number of nucleons participating in the collision, $\langle N_{part} \rangle$, the mean number of binary nucleon–nucleon collisions, $\langle N_{coll} \rangle$, the nuclear thickness function, $\langle T_{AA} \rangle$, as well as their uncertainties.

A particle emerging from the interaction point and passing through the inner detector typically crosses 4 layers of the pixel detector, 4 double-sided modules of the semiconductor tracker (SCT) and around 36 straw tubes of the transition radiation tracker. Reconstructed tracks are required to have at least 9 (11) hits, if they are within $|\eta| \leq 1.65$ ($|\eta| > 1.65$). At least one hit is required to be in one of the two innermost layers of the pixel detector, if the tracks passed through active sensors. Tracks shall not have any missing hits in the pixel or SCT detectors if such hits are expected from the track trajectory. Tracks are also required to emerge from the collisions vertex. Tracks with $p_T > 40$ GeV are further required to be matched to a jet within $\Delta R = \sqrt{\Delta^2\eta + \Delta^2\phi} < 0.4$. Jets are reconstructed with the anti-k_t algorithm [9] with the radius parameter of $R = 0.4$. Tracks are required not to exceed the p_T of the matched jets by more than 30% in order to suppress mis-measured tracks. They are suppressed by enforcing conservation of energy, however track and jet momentum resolutions are taken into account as well.

Monte Carlo simulations are used to study the detector response effects. Hard-scattering pp collisions generated by PYTHIA 8 [10] are overlaid onto Xe+Xe collisions produced by HIJING [11]. The resulting events are reconstructed in the same way as data. A total of $3 \cdot 10^6$ events are generated in different exclusive kinematic intervals of leading charged-hadron p_T, allowing sufficient statistics over the whole p_T range.

There are several corrections applied to the measured spectra. First, leptons from the decays of electroweak bosons are subtracted as they do not follow the same suppression pattern as hadrons [12]. Then, secondary and fake tracks are subtracted. The former ones are tracks matched to secondary particles, and the later ones are the tracks that are coming from the spurious combination of hits not associated with a single particle. Their fraction is estimated from the simulations. It does not exceed 1% at $p_T \approx 1$ GeV and is even less at higher p_T. The spectra are also corrected for the p_T resolution and for the track reconstruction efficiency by the bin-by-bin unfolding. The efficiency, which is also estimated from the simulations, is about 75% at $p_T \approx 1$ GeV, $|\eta| \lesssim 1$ and in peripheral collisions. At higher $|\eta|$, the efficiency decreases down to about 60%. Another reduction, which is less than 15%, is observed in the most central collisions. A small increase of the efficiency with increasing p_T is also present.

The pp cross-section measured at $\sqrt{s}$ = 5.02 TeV is extrapolated to $\sqrt{s}$ = 5.44 TeV by the ratio of the samples generated by PYTHIA 8 with $1.9 \cdot 10^7$ events in each energy regime. The ratio shows an increase of the cross-section section by about 4% at $p_T \approx 1$ GeV and up to 26% at the highest p_T and $|\eta|$ measured.

There are several sources of the systematic uncertainties affecting the results. The analysis parameters are varied independently and the resulting outcomes are compared to that of the default setup. The correlated components are varied consistently in numerator and denominator in order to estimate the uncertainty on R_{AA}. Variation of the track selection requirements introduces an uncertainty not exceeding 5%. The analysis corrections depend on a matching of the reconstructed tracks to the generated particles. The uncertainty covering ambiguities in the matching procedure is about 1%. The bin-by-bin correction uncertainty has

three sources. Limited statistics of the simulation samples yield an uncertainty of no more than 7%. The difference of the shape of charged-hadron spectra in data and PYTHIA results in an uncertainty of 2%. Due to the limited description of the inactive material of the detector, an uncertainty of up to 6% has to be assigned. An uncertainty of the geometric parameter $\langle T_{AA} \rangle$ is largest for the peripheral collisions where it reaches about 8%. In the central collisions, it is less than 1%. A half of the difference between the pp cross-sections at $\sqrt{s} = 5.02$ TeV and 5.44 TeV is assigned as a systematic uncertainty of the extrapolation.

3. Results

The left panel of Fig. 1 shows the nuclear modification factors, R_{AA}, for Xe+Xe and Pb+Pb collisions in the same centrality intervals. They have a characteristic curvature which is more pronounced in the central collisions. Curves reach a maximum at $p_T \approx 2$ GeV, then a minimum at around 7 GeV and then increase up to around 60 GeV. The behavior of R_{AA} in Xe+Xe collisions above this value is difficult to ascertain due to the low statistics. In Pb+Pb collisions, the slope of R_{AA} above $p_T \approx 60$ GeV diminishes. The stronger suppression in Pb+Pb than in Xe+Xe collisions for the same centrality intervals is expected because size of Pb+Pb collision system is larger than that of Xe+Xe collision. The right panel of Fig. 1 shows R_{AA}
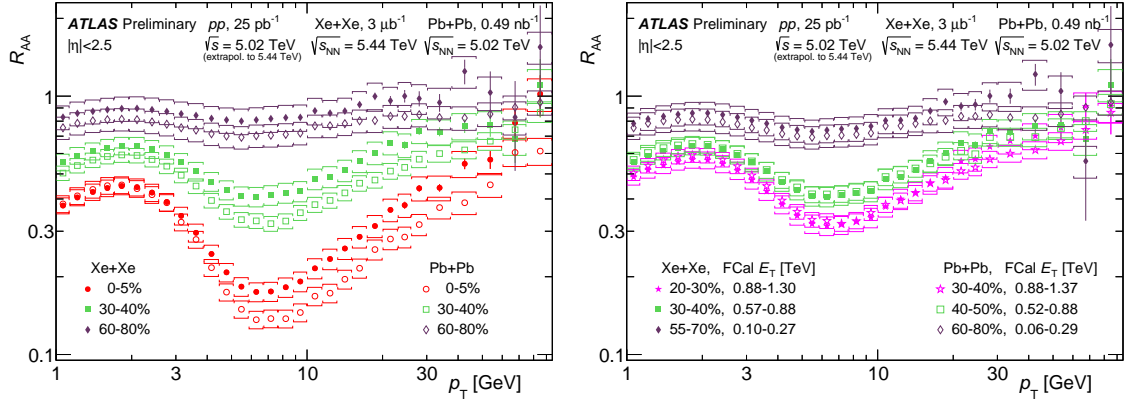

Fig. 1. Nuclear modification factors R_{AA} as a function of p_T measured in Xe+Xe collisions (closed markers) [5] and in Pb+Pb collisions (open markers) [4]. The intervals of the same marker styles have the same centrality (left) or comparable deposited energy in the forward calorimeter (right). The statistical uncertainties are shown as the bars; systematic uncertainties are shown by the brackets.
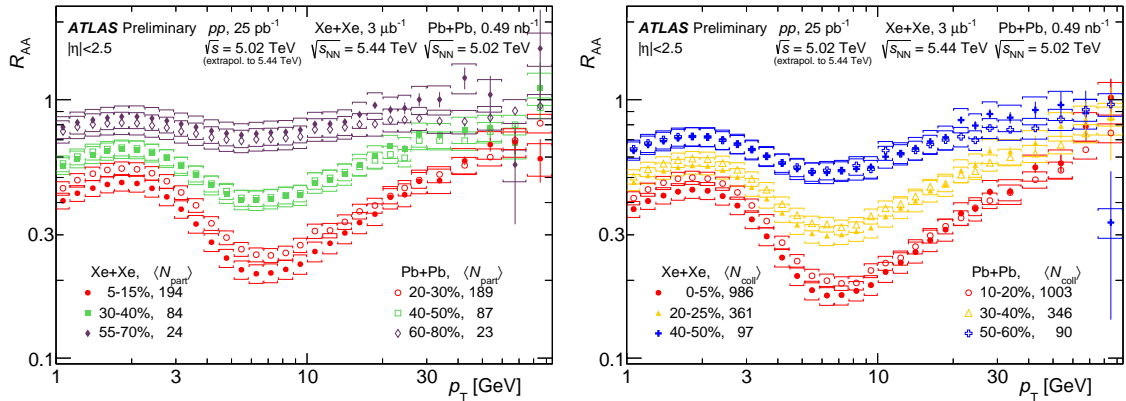

Fig. 2. Nuclear modification factors R_{AA} as a function of p_T measured in Xe+Xe collisions (closed markers) [5] and in Pb+Pb collisions (open markers) [4]. The centrality intervals of the same marker styles have comparable $\langle N_{part} \rangle$ (left) or $\langle N_{coll} \rangle$ (right). The statistical uncertainties are shown as the bars; systematic uncertainties are shown by the brackets.
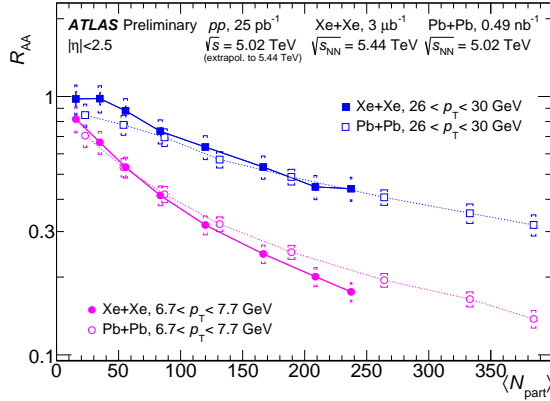
Fig. 3. Nuclear modification factors R_{AA} as a function of N_{part} for two selected p_T ranges measured in Xe+Xe collisions (closed markers) [5] and in Pb+Pb collisions (open markers) [4]. The statistical uncertainties are shown as the bars, and systematic uncertainties are shown by the brackets. The width of the brackets represents the systematic uncertainty of N_{part}. The lines are only to help guide the eye.

for Xe+Xe and Pb+Pb collisions in centrality intervals corresponding to approximately the same FCal E_T. Collisions with the same FCal E_T have about the same size. The observed suppressions are consistent between the two systems within the systematics uncertainties, suggesting scaling with the system size.

Figure 2 shows comparison of nuclear modification factors for Xe+Xe and Pb+Pb collisions for centrality intervals of similar $\langle N_{part} \rangle$ (left) and $\langle N_{coll} \rangle$ (right). The production rate of low-p_T (high-p_T) particles is proportional to N_{part} (N_{coll}), and therefore the size of the two systems is expected to be comparable at similar N_{part}. However, the agreement between the systems is still worse than in the right panel of Fig. 1. At low p_T, the Xe+Xe results show slightly stronger suppression for the central events, but slightly milder suppression for peripheral events. This feature is demonstrated in Fig. 3 where it is clearly visible. At higher p_T, the suppressions are comparable within uncertainties and R_{AA} measured in both Xe+Xe and Pb+Pb collisions follow the same dependency, which means the suppression scales with the system size.

4. Summary

Measurement of charged-hadron spectra and the nuclear modification factor in Xe+Xe collisions has been presented. The R_{AA} is compared between Xe+Xe data at $\sqrt{s_{NN}} = 5.44$ TeV and Pb+Pb data at $\sqrt{s_{NN}} = 5.02$ TeV measured by the ATLAS detector at the LHC. In spite of different geometry, the Xe+Xe and Pb+Pb data show similar suppression when the system sizes are comparable.

Acknowledgements

References

[1] G.-Y. Qin, X.-N. Wang, Int. J. Mod. Phys. E 24 (11) (2015) 1530014. arXiv:1511.00790 [hep-ph].
[2] Y. Mehtar-Tani, J. G. Milhano, K. Tywoniuk, Int. J. Mod. Phys. A 28 (2013) 1340013. arXiv:1302.2579 [hep-ph].
[3] ATLAS Collaboration, JHEP 09 (2015) 050. arXiv:1504.04337 [hep-ex].
[4] ATLAS Collaboration, ATLAS-CONF-2017-012. https://cds.cern.ch/record/2244824.
[5] ATLAS Collaboration, ATLAS-CONF-2018-007. https://cds.cern.ch/record/2318588.
[6] ATLAS Collaboration, JINST 3 (2008) S08003.
[7] M. L. Miller, et al., Ann. Rev. Nucl. Part. Sci. 57 (2007) 205–243. arXiv:nucl-ex/0701025.
[8] C. Loizides, J. Nagle, P. Steinberg, SoftwareX 1–2 (2015) 13–18. arXiv:1408.2549 [nucl-ex].
[9] M. Cacciari, G. P. Salam, G. Soyez, JHEP 04 (2008) 063. arXiv:0802.1189 [hep-ph].
[10] T. Sjöstrand, et al., Comput. Phys. Commun. 191 (2015) 159–177. arXiv:1410.3012 [hep-ph].
[11] X.-N. Wang, M. Gyulassy, Phys. Rev. D 44 (1991) 3501–3516.
[12] ATLAS Collaboration, ATLAS-CONF-2017-010. https://cds.cern.ch/record/2244821.